Baltimore, Maryland
NOISE-CON 2010
2010 April 19-21

An electroacoustic sound transmission system that is stable in any (dissipative) acoustic environment: An application of sound portholes

Edgar Berdahl[a)]
Berdahl Innovations
103 Cortland Ave.
San Francisco, CA 94110

Dan Harris[b)]
Sennheiser Research Laboratory
3239 El Camino Real, 3rd Floor
Palo Alto, CA 94306

Günter Niemeyer[c)]
Julius O. Smith III[d)]
Stanford University
Stanford, CA 94305

Active electroacoustic systems are commonly employed to transmit sound from one location to another. For example, consider the following configuration: a person talks into a microphone, which produces an electrically amplified signal for driving a loudspeaker, and the loudspeaker induces an output acoustic signal allowing someone else at a more distant location to hear the person talking. Unfortunately, such system designs typically do not consider acoustic feedback, which can destabilize the system and result in "howling." In contrast, a feedback control system can transmit sound from one location to another without the risk of howling using *sound portholes*, which are collocated microphone/loudspeaker transducers. We design feedback controllers to transmit sound between sound portholes. These controllers model physical analog systems, such as a spring or a gyrator. The spring controller essentially binds the diaphragms of the two sound portholes together. We relate the spring controller to the string connecting two tin cans in the classical tin can telephone. Measurements are performed on a real feedback control system with two sound portholes. Because the feedback controller models a passive system, it is theoretically stable in any (dissipative) acoustic environment.

[a)] Email address: eberdahl@ccrma.stanford.edu
[b)] Email address: Daniel.Harris@Sennheiser.com
[c)] Email address: gunter.niemeyer@stanford.edu
[d)] Email address: jos@ccrma.stanford.edu

1 INTRODUCTION

1.1 Overview

Electroacoustic systems are commonly employed to transmit sound from one location to another and/or to amplify sound. We show an example bidirectional sound transmission system in Figure 1. The person on the left speaks into a microphone, which sends an electrical signal to the amplifier with Laplace domain transfer function $K_2(s)$, which drives the loudspeaker accordingly (see Figure 1). The loudspeaker produces an output acoustic signal, typically to allow the person on the right to hear the speech. Similarly, the person on the right may speak through a microphone and the amplifier $K_1(s)$ to the person on the right. For convenience, we lump the frequency responses of the microphones and loudspeakers into $K_1(s)$ and $K_2(s)$. Since the amplifiers generate acoustical energy, there is the danger any acoustic feedback paths could employ this energy to drive the system unstable.

Nevertheless, during the initial design stages, engineers have usually ignored the acoustic feedback paths from the loudspeakers to the microphones. Figure 1 reveals that there are four different acoustic feedback paths. The local feedback paths $G_{12}(s)$ and $G_{21}(s)$ are the largest in magnitude; however, the feedback paths $G_{11}(s)$ and $G_{22}(s)$ are also capable of affecting the stability of the electroacoustic system. In many cases, the transducers can be placed and the magnitudes of $K_1(s)$ and $K_2(s)$ limited such that the acoustic feedback is indeed negligible and does not adversely affect the electroacoustic system. However, in other cases, the acoustic feedback can destabilize the system. For example, the reader is probably familiar with instances when someone on a stage placed a microphone too closely to a loudspeaker, causing the system to begin "howling" unpleasantly.

Researchers have provided some signal processing techniques for reducing such systems' tendency to howl[9,10], but these techniques cause some distortion of the amplified signal. Instead, the premise of this work is that we should study how to design electroacoustic feedback systems so that they are always guaranteed to be stable, regardless of transducer placement.

1.2 Overview

Consider the tin can telephone sound transmission system represented in Figure 2. When one of the persons speaks, the acoustic speech signal causes primarily the nearest disk to move. Then a string, modeled as a spring with stiffness k_C, connected to the disk causes the other disk to move in response. This disk actuates an acoustic wave for second person (see Figure 2) so that he or she can hear the speech. The system is bidirectional—each person can listen and talk at the same time.

The tin can telephone, also known as the lover's telephone, was invented as early as 1665. It can be constructed using two tin cans or paper cups connected together by a tensioned wire or string[7]. The wire behaves like a spring at sufficiently low frequencies, while the response becomes more complicated at higher frequencies due to longitudinal resonances of the string. Other similar prior devices include speaking tubes, which are air conduits employed for transmitting speech. Although superseded by telephones to a large degree, they can still be found on some ships.

The system shown in Figure 2 has some drawbacks. The sound transmission is especially limited in magnitude at low frequencies because disks radiate sound like dipoles at low frequencies. In addition, it is often physically inconvenient to run tensioned strings about a room, building, or city. However, the tin can system does not generate any energy, so it cannot become unstable. A system equivalent to the one shown in Figure 2 can be implemented, where a motor is attached to each disk, and the effect of the string is emulated using feedback control. In a more practical implementation, each disk is a collocated microphone/loudspeaker transducer, which we call a *sound porthole*. The sound portholes are bound together by a feedback control law emulating a spring with constant k_C. The controller is passive because of the existence of the mechanical analog shown in Figure 2—it is stable no matter where the sound portholes are placed or what the control system gain spring constant $k_C \geq 0$ is.

2 SOUND PORTHOLES

A sound porthole is a collocated microphone/loudspeaker device that can be constructed using a dual voice coil loudspeaker where the voice coils are wound over one another on the same bobbin[3-4]. It serves as a passive and bidirectional port connection between the acoustical and electrical domains. Beneath a certain impedance crossover frequency, the voltage across one coil is proportional to the velocity U of the bobbin, and the electrical current through the second coil is proportional to the force F exerted on the bobbin. In Figure 3, a person is shown interacting with a sound porthole, which is represented by a combination of the schematic symbols for a microphone and a loudspeaker.

We typically employ 8" (20.32cm) Quam 8C10DVPAXB dual voice coil loudspeaker drivers. The impedance crossover frequency is approximately 325Hz, and the mechanical resonance frequency is about 100Hz. Although we do not know the transducer's datasheet, we have estimated possible mechanical parameters given the mechanical resonance frequency of about 100Hz. The mechanical impedance due to the roughly estimated mass m, damping R, and stiffness k of the driver is shown in the dash-dotted red line in Figure 4. For comparison, the magnitude of the air loading $|Z_{al}(j\omega)|$ on the driver is plotted for comparison (see Figure 4, solid blue line). To estimate $Z_{al}(j\omega)$, we assume that each driver has a circular diaphragm with area A and is baffled by a rigid wall of infinite extent (see Figure 3.43[1]).

The Quam 8C10DVPAXB is a *loudspeaker* transducer, so as we expect, the magnitude of the transducer impedance is larger than the air load at most frequencies. However, near the 100Hz resonance frequency of the driver, we observe a dip in the transducer impedance beneath the air load. Near this region the impedances are well enough matched that the Quam 8C10DVPAXB responds well also as a microphone, so we expect the control system to operate well near and slightly above the resonance frequency.

3 MODEL

3.1 Without Control

In this section, we replace each disk shown in Figure 2 with an infinite array of sound portholes, and we calculate the transmission coefficient $T(s)$. For simplicity, we assume that an incoming sound pressure plane wave $P_{exc}(s)$ is impinging upon an infinite array of identical square sound portholes (see Figure 5, left). We assume that the sound portholes in the array

behave identically, meaning that the reflected sound pressure wave $P_1^-(s)$ is planar, and the sound pressure wave transmitted directly through the sound porthole $P_1^+(s)$ is also planar. One pair of portholes is highlighted, and the mechanical schematic for them is shown illustrating the mass m, damping R, and stiffness k. The velocity of the sound porthole highlighted on the left is $U_1(s)$ and on the right is $U_2(s)$ (see Figure 5).

The force due to the acoustic air pressure on each sound porthole is represented by the pressures multiplied by the surface area A of each sound porthole. Without control, the following two force balance equations would describe the dynamics of the two sound portholes:

$$\left(ms + R + 2Z_{al}(s) + \frac{k}{s}\right)U_1(s) = F_1(s) = \left(P_{exc}(s) + P_1^-(s) + P_1^+(s)\right)A \tag{1}$$

and

$$\left(ms + R + 2Z_{al}(s) + \frac{k}{s}\right)U_2(s) = F_2(s) = \left(P_2^-(s) + P_2^+(s)\right)A, \tag{2}$$

where $Z_{al}(s)$ represents the mechanical load placed on each sound porthole due to the air on one side of the infinite array. Since each sound porthole is acoustically loaded on both sides, the $Z_{al}(s)$ term is multiplied by two in (1) and (2). Because the air in contact with each sound porthole must have the same velocity as the sound porthole itself, we can also write:

$$Z_{al}(s)U_1(s) = \left(P_{exc}(s) - P_1^-(s)\right)A \qquad \text{and} \qquad Z_{al}(s)U_1(s) = -P_1^+(s)A. \tag{3}$$

Since we will calculate the transmission, we assume that the two infinite arrays of sound portholes are spaced infinitely far apart. Since there are no sound sources in between the infinite arrays, no waves impinge upon the sound portholes from the inside (see Figure 5). $P_2^-(s)$ and $P_2^+(s)$ are the sound pressure plane waves departing from the array of sound portholes on the right. Because the person shown on the right is not speaking, there is no wave traveling toward the array on the right from the right.

$$Z_{al}(s)U_2(s) = -P_2^-(s)A = -P_2^+(s)A \tag{4}$$

Finally, $P_{out}(s)$ is the portion of $P_2^+(s)$ that is radiated away from the sound portholes into the space to the right of the array on the right. Consequently, only the real part of the impedance $Z_{al}(s)$ is employed[1]:

$$\mathrm{Re}\{Z_{al}(s)\}U_1(s) = -P_{out}(s)A. \tag{5}$$

3.2 With Control

We test the effect of binding each pair of sound portholes together using a virtual spring with stiffness $k_C \geq 0$, a virtual damper with parameter $R_C \geq 0$, and a virtual gyrator with parameter l_C. The mechanical analogs of the controllers are shown for the highlighted sound portholes in Figure 6. Just like the spring, the damper and the gyrator are also passive (see Section 3.3). As long as either k_C, R_C or l_C is nonzero, an output plane wave $P_{out}(s)$ is transduced which depends on the input plane wave $P_{exc}(s)$. With control, the force balance equations (1) and (2) for each sound porthole change to the following:

$$\left(ms + R + 2Z_{al}(s) + \frac{k}{s}\right)U_1(s) = F_1(s) = P_{exc}(s)A + \left(R_C + \frac{k_C}{s}\right)(U_2(s) - U_1(s)) + lU_2(s) \tag{6}$$

and

$$\left(ms + R + 2Z_{al}(s) + \frac{k}{s}\right)U_2(s) = F_2(s) = \left(R_C + \frac{k_C}{s}\right)(U_1(s) - U_2(s)) - lU_1(s). \tag{7}$$

Finally, by substituting (3) and (7) into one another, we can find the transmission coefficient:

$$T(s) = \frac{P_{out}(s)}{P_{exc}(s)} = \frac{-2 \cdot \mathrm{Re}\{Z_{al}(s)\} \cdot (R_C + \frac{k_C}{s} - l)}{\left(ms + (R_C + R) + (\frac{k_C}{s} + \frac{k}{s}) + 2Z_{al}(s)\right)^2 - (\frac{k_C}{s} + R_C + l)(\frac{k_C}{s} + R_C - l)}. \quad (8)$$

3.3 Transmission Limit

Large $|T(j\omega)|$ are desirable in this application. Since we are designing passive controllers, we cannot have $|T(j\omega)|>1$, which would correspond to amplification. The magnitude of the maximum achievable transmission coefficient is further reduced by the presence of the waves $P_1^+(s)$ and $P_2^-(s)$, which are unnecessary for this application. Hence, at best the array shown on the left in Figure 6 can completely absorb the incoming wave $P_{exc}(s)$, using it to induce the waves $P_{out}(s)$ and $P_2^-(s)$. However, for our application, we only require $P_{out}(s)$. Intuitively, the transmission magnitude

$$|T(j\omega)| \leq 1/2 \quad (9)$$

for the current model. Clearly it would be preferable to achieve a larger $|T(j\omega)|$. We could achieve a bound of 1 instead of 1/2 by eliminating the air between the drivers shown in Figure 6. This measure would force $P_1^+(s)=P_2^-(s)=0$. However, it is difficult in practice to place a vacuum on one side of a sound porthole. Nevertheless, it might be possible to approximate this condition at some frequencies by baffling each sound porthole individually with a small, sealed box. The stiffness of the air would increase the sound porthole natural stiffness k, increasing the resonance frequency and thus the range over which the sound portholes operate well.

4 EXPERIMENT

4.1 Hardware

To demonstrate the feasibility of employing passive feedback control using mechanical analogs for constructing electroacoustic transmission systems, we employed a prototype consisting of two sound portholes, two current-drive power amplifiers, and a low-latency digital feedback controller. The controller was implemented using the Sennheiser "ZAMP" digital signal processing (DSP) research platform, which incorporates an Analog Devices SHARC floating point DSP. The controller was programmed to emulate the spring k_C, gyrator l_C, and damper R_C shown in Figure 6. The sampling rate f_S=48kHz, and the total system delay was about 30μs, which included $1/(2f_S)\approx$10μs due to the nature in which a zero-order hold delays a control signal[5].

4.2 Increasing Feedback Level Can Inhibit Howling

We present an example with the gyrator to demonstrate the advantage of collocated, passive feedback control. Figure 7 shows the signal flow diagram of two sound portholes coupled together by a gyrator with coefficient l_C. The sound portholes are also coupled by the transfer function $G_{12}(s)$ through the air. Due to the reciprocity theorem[1], the transfer function must be the same in each direction, so it is drawn only once but with double-ended arrows (see the dash-dotted red lines in Figure 7). The people depicted do not take part in this experiment, but they are drawn to emphasize the relation to the system shown in Figure 1. Each of the blocks labeled *Pwr* is a current-controlled power amplifier that converts a commanded force signal into a

current for driving a sound porthole. The gyrator with parameter l_C implements the following control law:

$$F_1 = l_C U_2 \quad \text{and} \quad F_2 = -l_C U_1. \tag{10}$$

The gyrator is passive because the sum of the power flowing into the portholes is equal to zero, regardless of the value of l_C:

$$F_1 U_1 + F_2 U_2 = (l_C U_2)\frac{F_2}{-l_C} + F_2 U_2 = -F_2 U_2 + F_2 U_2 = 0. \tag{11}$$

Because the gyrator does not generate any energy, it cannot drive the sound portholes and coupled acoustic system unstable. Hence, given an ideal implementation of the system shown in Figure 7, the control gain l_C could be made arbitrarily large without affecting the stability of the control system. We added a switch to the signal flow diagram in Figure 7, which made it possible to mute the control force acting on the first sound porthole. We placed two sound portholes in the laboratory near one another as shown in Figure 8.

• In the *muted* condition, the system began to howl as the control system became nonpassive violating (11) since F_1=0. Figure 7 depicts the only remaining feedback loop in dashed lines.

• In the *unmuted* condition, the control system operated passively as designed, and any howling oscillations quickly died out.

Figure 9 shows an example recording of the current $i_2(t)$ powering the second sound porthole. At the beginning of the sample, the control power to the first sound porthole is muted, so the system howls. At time t=3.5s, the control power to the first sound porthole is unmuted, causing the howling oscillation to quickly die out. At time t=6.5s, the control power to the first sound porthole is again muted, causing the electroacoustic transmission system to again become unstable and start howling. Note that this is an example where *INCREASING the feedback level can INHIBIT howling.* Thus, we argue that in some applications, a bidirectional passive connection inspired by analog mechanical systems is better than one or two nonpassive unidirectional systems, which can howl.

4.3 Transmission

We measured the transmission coefficient of the system we implemented. An ADAM A7 loudspeaker was placed 3" (7.6cm) away from the first sound porthole to simulate $P_{exc}(s)$. Similarly, an AKG C 460B microphone body with CK62-ULS capsule (roll-off switch disabled) was placed 3" (7.6cm) away from the second sound porthole. The transfer function from the ADAM A7 to the microphone was measured for the spring, gyrator, and damper. These transfer functions were normalized by the direct transfer function measured with the microphone alone placed 6" (15.2cm) directly in front of the ADAM A7 on axis. The thusly normalized transmission magnitudes $|T(j\omega)|$ for the three different kinds of controllers are shown in Figure 10. As expected, each controller induced significant transmission in a region above the sound porthole resonance frequency of 100Hz. This was the region where the impedance match between the transducer parts and the acoustical air load was best (see Figure 4).

The transmission of all of the passive controllers was limited by the 1/2 (-6dB) limit derived in Section 3.3. This limit is shown in large, magenta circles in Figure 10. The transmission coefficient magnitude appears to have exceeded -6dB slightly at some frequencies, but we

believe that this was an artifact of not performing the measurement in an anechoic chamber. In other words, acoustic reflections made the measurement-based estimation of $T(j\omega)$ non-ideal.

The spring controller due to k_C caused the resonance frequency mode of the sound porthole to split into two modes; one remained near 100Hz, and the other increased to somewhere near 300Hz. Increasing the value of k_C increased the amount of splitting. The transmission for the spring ranged over a fairly large band; and its magnitude was relatively large (see blue, thin solid line in Figure 10). The damper controller R_C performed similarly; however, since it dissipated energy, the transmission was reduced slightly (see the black, thin dashed line in Figure 10). The "gyrator" measurement was performed using l_C with a slight amount of damper characteristic R_C. This controller induced transmission up to the -6dB limit but was especially bandlimited to a region near 180Hz (see the red, thick dash-dotted line in Figure 10). Increasing l_C caused the frequency of this region to increase, while the level remained approximately constant for moderate values of l_C.

5 CONCLUSIONS

In some applications, a bidirectional electroacoustic system, such as the one shown in Figure 7, which is inspired by a mechanical analog system, is better than one or two unidirectional systems, such as the systems shown in Figure 1, which can howl. Further research in this area is warranted for learning how to fully leverage the advantages of feedback control using mechanical analog controllers.

The spring, gyrator, and damper controllers can be used to induce sound transmission between sound portholes. However, the transmission is bandlimited as shown by the gyrator, spring, and damper transmission coefficient magnitudes in Figure 10. More complex mechanical analog controllers are needed to optimize the bandwidth and magnitude of the transmission coefficient level $|T(j\omega)|$. Such controllers would consist of multiple springs, dampers, masses, and gyrators[2].

Since the control system naturally performs best in a frequency region above the sound porthole resonance frequency, any practical implementation would need to incorporate separate transducers for controlling separate frequency regions. The 1/2 (-6dB) transmission described in Section 3.3 could be at least partially overcome with acoustical transducer designs that limit the acoustical loading on the transducer.

In addition, collocated dual voice coil transducers are needed that have lower transducer part impedances, and hence are better matched to the air. To some extent, feedback control can be employed to reduce the transducer part impedances, for instance reducing the mass m or stiffness k, but the best solution is to alter the mechanical properties of the transducers themselves. Horns could likely also be employed advantageously[1]. We look forward to constructing new drivers in order to satisfy these requirements.

6 ACKNOWLEDGEMENTS

We wish to graciously thank Sennheiser Electronic Corporation for supporting this work. We would like to also especially extend our gratitude to Veronique Larcher for her assistance.

7 APPENDIX: RELATION TO FEEDBACK CONTROL THEORY

We introduce some concepts from the field of feedback control and relate them to the theme of the paper. It is easiest to introduce these concepts using a single-input single-output system, such as the traditional electroacoustic amplification system shown in Figure 11. *K(s)* incorporates the microphone and loudspeaker transducer responses as well as the amplifier transfer function. *G(s)* represents the acoustic feedback path. The Revised Bode Stability Criterion states the following:

> A linear and time-invariant single-input single-output closed-loop system is stable if the open-loop transfer function *G(s)K(s)* is stable and the frequency response of the open-loop transfer function has an amplitude ratio of less than unity at all frequencies corresponding to an angle of $-\pi-n(2\pi)$, where $n=0,1,2,...,\infty$.[6]

The criterion implies that if the phase lag introduced by *K(s)* and *G(s)* is small enough, then the system shown in Figure 11 will be stable no matter how large the loop gain is. Expressed mathematically, the system is stable if *K(s)* is *positive real* and *G(s)* is *strictly positive real*. However, *G(s)* cannot be strictly positive real if it includes any delay. In other words, in order for *G(s)* to be strictly positive real, and similarly to keep the phase lag bounded at high frequencies, **the microphone and loudspeaker need to be placed at the same position in space, i.e., they need to be *collocated***[2,8]. The configuration shown in Figure 11 prevents *G(s)* from being strictly positive real because of the acoustic delay between the loudspeaker and the microphone.

We now assume that all microphones and loudspeakers are collocated and matched. Then it follows that *K(s)* is positive real if and only if *K(s)* corresponds to a passive mechanical analog system, and *G(s)* is strictly positive real if and only if it corresponds to a dissipative mechanical analog system. In summary, the control system is guaranteed to be stable if **the controller transfer function *K(s)* is passive and the plant transfer function *G(s)* is dissipative.** In other words, *K(s)* may not add any energy to the control system, and *G(s)* must remove energy from the control system at all frequencies. This important property explains why researchers in the active control of structural vibrations often use passive controllers *K(s)*[8]. In theory, the loop gain may be then made arbitrarily large implying that a large amount of control power can be exerted. In practical implementations, other limits come into play, but nonetheless, passive controllers tend to be especially useful in practice.

The restrictions shown in boldface above prevent us from implementing many electroacoustic systems, such as the one shown in Figure 11. Nevertheless, it is possible to implement some useful electroacoustic systems adhering to the restrictions such as the system shown in Figure 6. To satisfy these restrictions in the course of this paper, we have chosen

controllers *K(s)* that correspond to mechanical analogs, and we have connected the controllers to the air using collocated sound portholes to form dissipative *G(s)*.

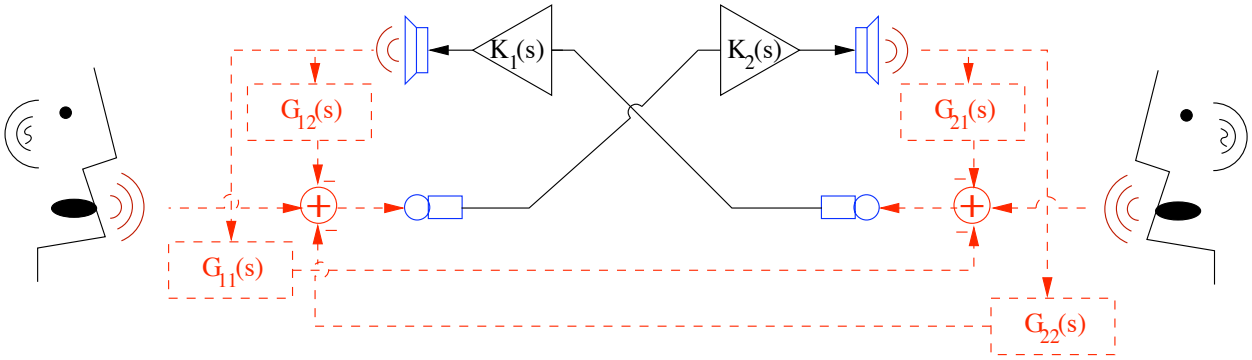

Fig. 1 - Bidirectional sound transmission system with power amplifiers $K_1(s)$ and $K_2(s)$ and acoustic feedback transfer function paths shown in dashed red lines.

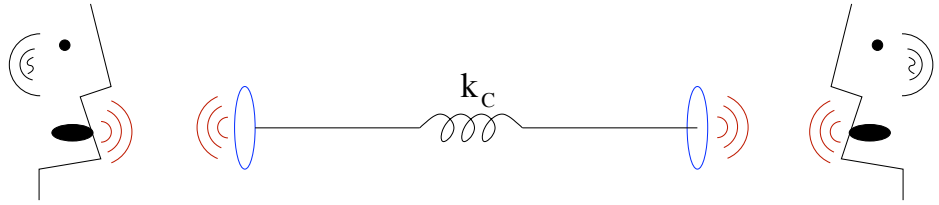

Fig. 2 - Simplified model of the tin can telephone sound transmission system.

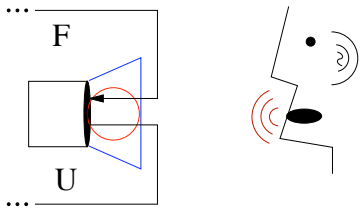

Fig. 3 - Person interacting with a sound porthole with velocity U and control force F.

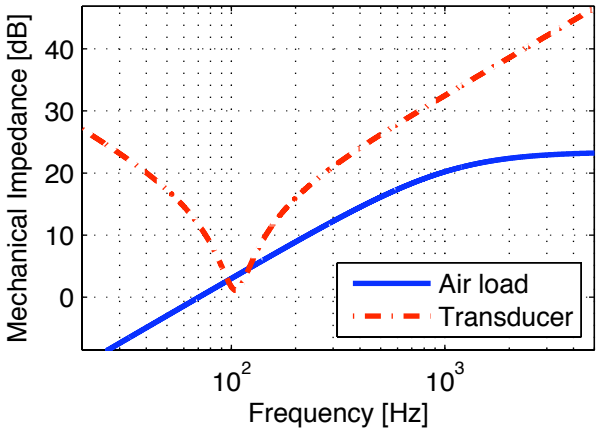

Fig. 4 - Sound porthole impedance magnitude due to the air load $|Z_{al}(j\omega)|$ (solid blue) and due to the transducer parts $|m(j\omega) + R + k/(j\omega)|$ (dash-dotted red).

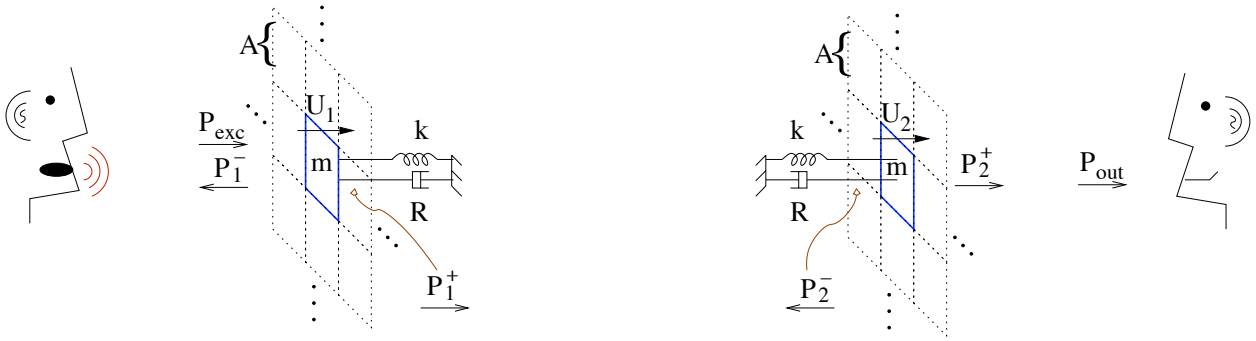

Fig. 5 - Plane wave model describing two infinite walls of sound portholes without feedback control.

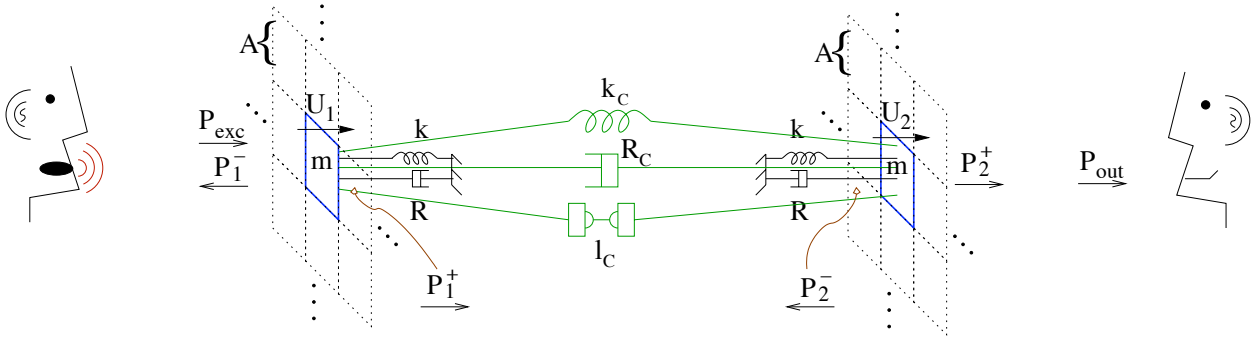

Fig. 6 - Plane wave model describing two infinite walls of sound portholes with feedback control mechanical analogs shown in green for transmitting sound pressure waves.

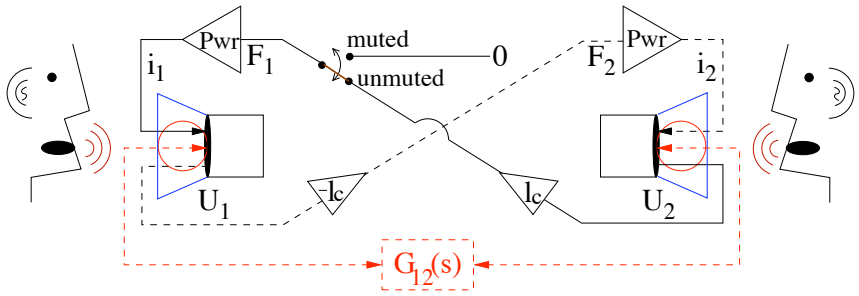

Fig. 7 - Signal flow diagram for gyrator with mute switch for one channel.

Fig. 8 - Two sound portholes placed near one another.

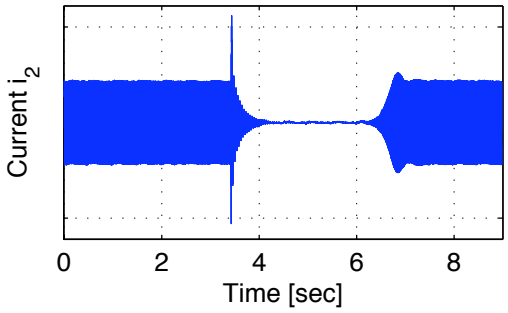

Fig. 9 - Current $i_2(t)$ powering the second sound porthole for demonstrating that increasing the level of feedback can inhibit howling in some situations.

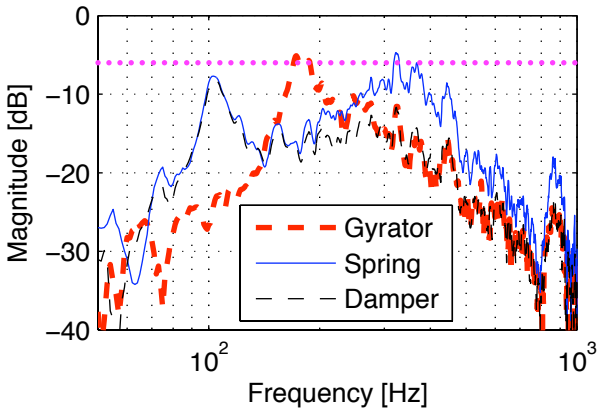

Fig. 10 - Transmission coefficient magnitude $|T(j\omega)|$ for the gyrator (red, thick dashed line), the spring (blue, thin line), and the damper (green, thin dashed line).

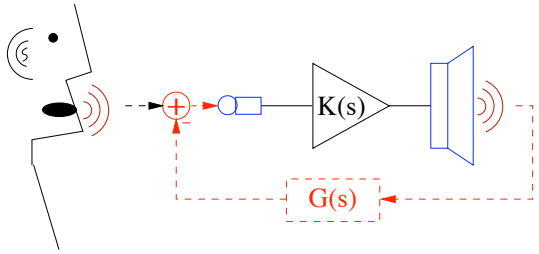

Fig. 11 - Person speaking into a microphone, whose signal is processed by an amplifier with transfer function K(s) and fed to a loudspeaker; acoustic path from loudspeaker to microphone represented by G(s).

8 REFERENCES

1. Leo Beranek. *Acoustics*. Acoustical Society of America, Woodbury, NY, (1993).

2. Edgar Berdahl. *Applications of Feedback Control to Musical Instrument Design*, PhD thesis, Stanford University, Stanford, CA, USA, January (2010).

3. C. Chen, G. Chiu, C. Cheng, and H. Peng. "Passive voice-coil feedback control of closed-box subwoofer systems," *Journal of Mechanical Engineering Science (Part C)*, **214**:995–1005, (2000).

4. Egbert De Boer. "Theory of motional feedback," *IRE Transactions on Audio*, **9**(1):15–21, (1961).

5. Gene Franklin, J. Powell, and Abbas Emami-Naeini. *Feedback Control of Dynamic Systems*, Prentice Hall, Fifth edition, (2005).

6. Jürgen Hahn, Thomas Edison, and Thomas Edgar. "A note on stability analysis using bode plots," *Chemical Engineering Education*, **35**(3):208–211, (2001).

7. Robert Hooke. Preface to *Micrographia: or, Some physiological descriptions of minute bodies made by magnifying glasses.* J. Martyn and J. Allestry, London, England, First Edition, (1665).

8. Marty Johnson and Stephen Elliott. "Active control of sound radiation using volume velocity cancellation.," *Journal of the Acoustical Society of America*, **98**(4):2174–2186, October (1995).

9. James Kates. "Feedback cancellation in hearing aids: Results from a computer simulation," *IEEE Transactions on Signal Processing*, **39**(3):553–562, March (1991).

10. Manfred Schroeder. "Improvement of acoustic-feedback stability by frequency shifting," *Journal of the Acoustical Society of America*, **36**(9):1718–1724, September (1964).